climate

MDPI

Article

The Value of Tactical Adaptation to El Niño–Southern Oscillation for East Australian Wheat

Bangyou Zheng [1], Scott Chapman [1,2] and Karine Chenu [3,*]

1 CSIRO Agriculture and Food, Queensland Bioscience Precinct, 306 Carmody Road, St. Lucia, QLD 4067, Australia; bangyou.zheng@csiro.au (B.Z.); scott.chapman@csiro.au (S.C.)
2 School of Agriculture and Food Sciences, The University of Queensland, Building 8117A NRSM, Gatton, QLD 4343, Australia
3 The University of Queensland, Queensland Alliance for Agriculture and Food Innovation (QAAFI), 203 Tor Street, Toowoomba, QLD 4350, Australia
* Correspondence: Karine.Chenu@uq.edu.au; Tel.: +61-(0)7-4688-1357

Received: 6 August 2018; Accepted: 8 September 2018; Published: 11 September 2018

Abstract: El Niño–Southern Oscillation strongly influences rainfall and temperature patterns in Eastern Australia, with major impacts on frost, heat, and drought stresses, and potential consequences for wheat production. Wheat phenology is a key factor to adapt to the risk of frost, heat, and drought stresses in the Australian wheatbelt. This study explores broad and specific options to adapt wheat cropping systems to El Niño–Southern Oscillation, and more specifically, to the Southern Oscillation Index (SOI) phases ahead of the season (i.e., April forecast) in Eastern Australia, when wheat producers make their most crucial management decisions. Crop model simulations were performed for commercially-grown wheat varieties, as well as for virtual genotypes representing possible combinations of phenology alleles that are currently present in the Australian wheat germplasm pool. Different adaptation strategies were tested at the site level, across Eastern Australia, for a wide range of sowing dates and nitrogen applications over long-term historical weather records (1900–2016). The results highlight that a fixed adaptation system, with genotype maturities, sowing time, and nitrogen application adapted to each location would greatly increase wheat productivity compared to sowing a mid-maturity genotype, mid-season, using current practices for nitrogen applications. Tactical adaptation of both genotype and management to the different SOI phases and to different levels of initial Plant Available Water ('PAW & SOI adaptation') resulted in further yield improvement. Site long-term increases in yield and gross margin were up to 1.15 t·ha^{-1} and AU$ 223.0 ha^{-1} for fixed adaptation (0.78 t·ha^{-1} and AU$ 153 ha^{-1} on average across the whole region), and up to an extra 0.26 t·ha^{-1} and AU$ 63.9 ha^{-1} for tactical adaptation. For the whole eastern region, these results correspond to an annual AU$ 440 M increase for the fixed adaptation, and an extra AU$ 188 M for the PAW & SOI tactical adaptation. The benefits of PAW & SOI tactical adaptation could be useful for growers to adjust farm management practices according to pre-sowing seasonal conditions and the seasonal climate forecast.

Keywords: ENSO; Southern Oscillation Index; SOI; El Niño; La Niña; soil water; environment type; climate adaptation; management practices; crop model; APSIM

1. Introduction

In Australia, the wheat industry is challenged by complex genotype x environment x management (GxExM) interactions [1,2], due in part to the high spatial and temporal variability of the Australian climate (e.g., [3]). In the eastern part of the continent, annual variations in temperature and rainfall that are influenced by El Niño–Southern Oscillation (ENSO) [1,4,5] affect frost, heat, and drought

stress patterns [5–7], and ultimately, wheat production [1,3,5]. Drought and warmer temperatures, but also greater frost risk due to the clear night sky, are generally associated with the onset of El Niño episodes [5,8,9], and limit grain yield [10–13]. Stronger ENSO climate oscillations are expected in the near future, as climate forecasts project more frequent extreme El-Niño and La-Niña conditions [14,15].

As the major driver of inter-annual climate variability in Eastern Australian [4,5,16], ENSO is a quasiperiodic climate pattern that occurs across the tropical Pacific Ocean every 3–8 years. It is caused by variations in the surface temperature of the tropical eastern Pacific Ocean, and the air surface pressure in the tropical western Pacific [17]. The Southern Oscillation Index (SOI), as measured by surface pressure anomaly difference between Tahiti and Darwin, has been used to investigate ENSO effects on crops. Five SOI phases have been defined through grouping all sequential two-month pairs of the SOI into five clusters, using principal component analysis and a cluster analysis [18]. Hammer et al. [1] found that using the 5-phase SOI classification (based on SOI values for the current and previous month) could significantly increase wheat profits (up to 20%) and decrease failure risk (up to 35% less risk) in Goondiwindi, South-Eastern Queensland, Australia, through adapting wheat cultivars and nitrogen fertiliser.

Strategies for yield improvement include breeding new cultivars and adapting management practices to the target population of environments [19]. Climate forecasting offers new opportunities in terms of agricultural planning and operation [4]. In the Australian broad-acre dryland wheat production area, most major decisions occur prior to sowing. Producers can potentially react to early indicators of upcoming rainfall and temperature. Early estimation of SOI phases can thus help farmers adjust management practices such as which cultivar to sow, when to sow, and what nitrogen fertilisation to apply [5,20,21].

In Eastern Australia, wheat crops rely heavily on soil-stored plant available water (PAW) [6,22]. An appropriate combination of sowing data, variety maturity, and pre-sowing PAW is crucial to allow flowering and grain filling to occur with minimal stress, in particular frost, heat, and drought stress, and thus, to maximise yield potential [6,7,23–25]. In this context, crop modelling can assist farmers to adapt their practices to specific SOI phases through adequate choice of maturity type and sowing date, in order to get extra benefit and increased profit [26].

The aims of this paper were to determine the values of (i) fixed adaptation (no distinction between the years) and (ii) adaptations to specific pre-sowing plant available water (PAW) and/or SOI phase. In this study, adaptation strategies were defined in terms of sowing, maturity type, and nitrogen fertilisation, to target the greatest long-term productivity at each site. The APSIM crop model [27], together with a phenology model [28], frost impact module [12] and heat impact module [10], were used to predict flowering time and yield of wheat, and search for the best long-term adaptation strategies.

2. Materials and Methods

2.1. Climatic Data

Fifteen weather stations representing local pedo-climatic conditions from the East Australian wheatbelt [7,22] were selected (see Chenu et al., 2013 [22] for more details) to compare adaptation options to Southern Oscillation Index (SOI) phases (Figure 1, Table 1).

The SOI, which corresponds to differences in sea level pressure between Tahiti and Darwin, has been classified in five phases [18]: 'consistently negative' (I), 'consistently positive' (II), 'rapidly falling' (III), 'rapidly rising' (IV) and 'consistently near zero' (V). These phases were grouped into three classes: consistently negative and rapidly falling (SOI phases I & III), consistently positive and rapidly rising (SOI phases II & IV), and consistently near zero (SOI phase V), as suggested by Potgieter et al. [3]. Weather records from 1900 to 2016 (117 years) were extracted from the Australian weather database (SILO Patched Point Dataset [29]; http://www.longpaddock.qld.gov.au/silo/). The SOI phase classification was sourced from Seasonal Climate Outlook in the Long Paddock (http://www.longpaddock.qld.gov.au/). In this study, the SOI phases were classified using SOI

values from March–April to look at the effects for a pre-season indicator. From 1900 to 2016, 36 years had been classified as SOI phases I & III, 45 years as SOI phases II & IV and 34 years as SOI phase IV.

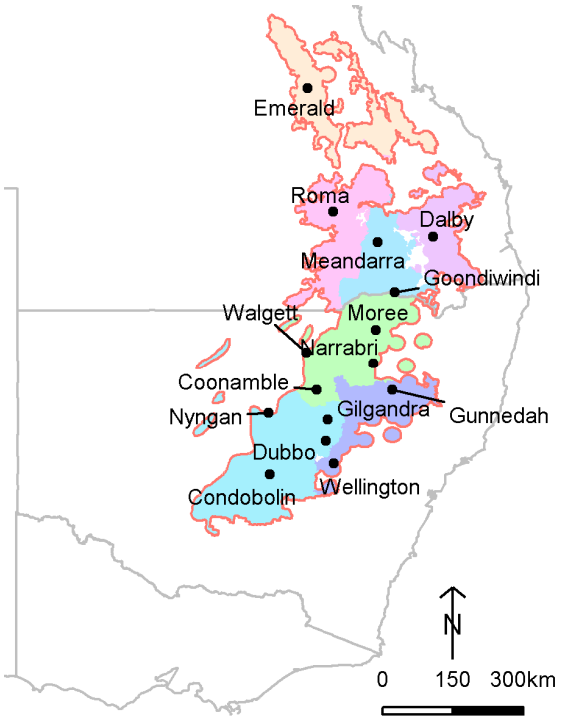

Figure 1. Map of the seven regions of the East Australian wheatbelt, with 15 sites chosen to represent those regions. Details on the locations can be found in Chenu et al., 2013 [22].

Table 1. Regions, locations, soil nitrogen at sowing and nitrogen fertilisation (in the baseline simulations), minimum pant available water (PAW) at sowing chosen to represent the East Australian wheatbelt. Initial and applied nitrogen (N) is indicated by 'x-y-z-a': x, initial N present in the soil at sowing; y, N applied at sowing as urea; z and a, N applied as nitrate at the stages 'beginning of stem elongation' and 'mid-stem elongation', respectively.

Region	Location	Lat.	Long.	Nitrogen (kg ha^{-1})	Minimum PAW at Sowing (mm)
Central Queensland	Emerald	−23.53	148.16	30-50-0-0	80
Eastern Darling Downs	Dalby	−27.18	151.26	30-130-0-0	80
Eastern NSW	Gunnedah	−30.98	150.25	50-70-60 *-0	80
	Wellington	−32.80	148.80	50-50-50 †-0	50
Northern NSW	Moree	−29.48	149.84	30-80-0-0	80
	Walgett	−30.04	148.12	30-80-0-0	80
	Narrabri	−30.32	149.78	30-130-0-0	80
	Coonamble	−30.98	148.38	50-70-60 †-0	50
Southern West Queensland	Roma	−26.57	148.79	30-50-0-0	80
Western Darling Downs	Meandarra	−27.32	149.88	30-80-0-0	80
	Goondiwindi	−28.55	150.31	30-80-0-0	80
Western NSW	Nyngan	−31.55	147.2	50-60-60 †-0	80
	Gilgandra	−31.71	148.66	50-50-50 †-0	50
	Dubbo	−32.24	148.61	50-50-50 †-0	50
	Condobolin	−33.07	147.23	50-60-60 †-0	80

* >80 mm of rainfall from sowing to the stage "end of tillering–beginning of stem elongation". † >100 mm of rainfall from sowing to the stage "end of tillering–beginning of stem elongation".

Monthly temperature and cumulated rainfall were calculated as the average for each month from 1900 to 2016. Daily minimum and maximum temperatures were used to determine occurrences of frost and heat events.

2.2. Crop Simulations and Gross Margins

Wheat yield (dry weight without moisture content) was simulated for the 15 sites (Figure 1, Table 1) from 1900 to 2016. The simulations were performed with the APSIM 7.5 model [27,30], which has been widely tested for wheat across Eastern Australia (e.g., Chenu et al., 2011; Holzworth et al., 2014; Christopher et al., 2016 [6,27,31]; http://www.apsim.info/APSIM.Validation/Main.aspx), and a wheat-phenology gene-based module [28], a heat impact module [10], and a frost impact module with a frost-stress threshold of −2 °C [12].

For each site and year, the simulations were begun with a summer fallow starting from 1 November with a soil containing 20% of its potential available soil water capacity (PAWC). Wheat crops were sown at two-day intervals within a fixed sowing window from the 1 April to 30 June for all 15 sites, when the soil held enough plant available water (PAW) at sowing (Table 1). Soil nitrogen and surface organic matter were reset at sowing. The base nitrogen fertilisation was chosen to reflect local farming practices, and therefore, varied with site and seasonal rainfall, as defined in Chenu et al., 2013 [22] (Table 1). Plants were grown at a density of 100 plants per m^2. Seasons with not enough soil water on 1 April (i.e., when management options were chosen for the tactical adaptation scenarios, see below) were excluded from the analysis.

Different management strategies were tested with a range of sowing dates (sowing every two days from 1 April to 30 June) and nitrogen applications. An extra 0 to 140 kg·ha^{-1} (at 20 kg·ha^{-1} interval) of nitrogen was applied to the base simulations. Nitrogen fertilisation was applied at the same stage(s) as in the base simulations (i.e., local farming practices) with the same proportions, i.e., at sowing and/or 'beginning of stem elongation' depending on the seasonal opportunities.

Simulations were performed for 208 genotypes including commercial varieties and virtual genotypes that could potentially be bred based on the flowering alleles present in the Australian germplasm pool (see Zheng et al., 2013 for details [28]). Virtual genotypes were created including all combinations of *VRN-A1*, *VRN-B1*, *VRN-D1*, and *PPD-D1* genes (two alleles for each gene), and the full range of values of additional thermal time requirement from floral to flowering (from 425 to 1025 °Cd [28]). Genotypes with the same phenology (from different allelic combinations) were disregarded, so that a total of 156 genotypes unique for their phenology were considered. Overall, the selected genotypes had APSIM parameters ranging from 0 to 1.2 for the photoperiod sensitivity (0.6 for the reference genotype Janz), 0.9 to 1.7 for the vernalisation sensitivity (0.9 for Janz), and 425 to 1025 °Cd for the additional thermal time requirement from floral to flowering (675 °Cd for Janz).

Odd and even years were first simulated separately as some crops matured after 1 November (date of the simulation initialisation). Odd- and even-year simulations were then merged together. Overall, 800 thousand simulations were run through the CSIRO HTCondor service using ClusterRun platform with the runs being completed in less than 4 h [32].

The gross margin was estimated for each simulation based on wheat and nitrogen prices. Other costs of wheat production were ignored, as only variations in gross margin were considered in this study (i.e., only the fertilisation costs varied among the tested management options). The wheat and nitrogen (as urea) prices were sourced from Australian Commodity Statistics [33], and calculated as median values from 2003 to 2012 (i.e., AU$ 269 and AU$ 547 per tonne for wheat and urea, respectively). Variation in grain quality was not considered in this study as the APSIM-wheat model is currently not able to accurately simulate changes in wheat protein content. Increase in gross margin at each site was multiplied with the planting area of the considered region (averaged data from 1975 to 2000, 2004 and 2006; source: Australian Bureau of Statistics), and all regional values were summed to obtain the total increase in gross margin for the Eastern region. Hence, gross margin estimations did not account for changes in fertilizer prices, changes in planting area, changes in wheat prices related to the harvested grain quality, nor changes in wheat prices related to fluctuations in the domestic and/or global market.

2.3. Fixed and Tactical Adaptation Options

Different scenarios exploring the GxExM interactions were evaluated to test their values for different pre-sowing levels of soil water and/or for the three different SOI classes at each studied site. The acceptable range of soil PAW (from minimum required PAW at sowing (Table 1) to the PAWC) calculated at 1 April was divided into three groups (0–33%, 33–67%, 67–100%) to represent Low, Median and High pre-sowing water levels. The 156 genotypes unique for their phenology were considered, as well as sowing dates from 1 April to 30 June and different nitrogen fertilisation options (see previous section).

To provide a reference against conventional practice, a baseline scenario was defined. In this scenario, the reference cultivar Janz was simulated from 1900 to 2016 for a sowing at 21 May using standard farmer practices for fertilisation (Table 1) [22]. A strategic 'fixed scenario' that considers the best management and best genotype for all years (in terms of highest average yield) at each location ('Fixed adaptation') was used as benchmark for best long-term practices (1900–2016). To investigate the potential tactical advantages of adapting, whereby a grower would modify planting decisions based on the SOI phases and/or soil PAW prior to sowing, scenarios with optimised genotypes and management practices specific to SOI classes and/or PAW groups were defined (at each location) through maximizing the average yield for crops grown within each SOI class and/or PAW group. For each location, the tactical adaptation scenarios consisted in either (1) the 'PAW' scenario, which considered the best overall genotype and management within situations from each PAW group, (2) the 'SOI' scenario, which considered the best overall genotype and management within situations from each SOI class, or (3) the 'PAW & SOI' scenario where both genotype and management were optimised for each combination of PAW group × SOI class. For the different scenarios, yield differences and changes in gross margin compared to the baseline and fixed adaptation scenarios were calculated for each year.

3. Results and Discussion

3.1. SOI Impacts on Seasonal Temperature and Rainfall

In the Eastern wheatbelt, SOI phases from the end of summer (calculated in March–April) were typically associated with temperature and cumulated rainfall recorded during the 'summer' fallow preceding the wheat crop (November to April). Higher temperatures were recorded for years with consistently negative SOI (phase I), and to a lesser extent, for years with rapidly falling SOI (III), while lower temperatures occurred in years with consistently positive SOI (II), and to a lesser extent, in years with rapidly increasing SOI (IV) (data not shown, Figure 2A and Figures S1–S3). For instance, the temperature in years from SOI phase I was up to 1.5 °C higher than the 'all years' data in February and March in Emerald, Roma and Gunnedah (data not shown). By contrast, summer rainfall tended to be lowest for SOI phases I & III, and highest for SOI phases II & IV (Figure 2B and Figure S7). As wheat crops in the Eastern wheatbelt heavily rely on soil-stored plant available water (PAW) [6,22], this implies that differences observed in summer rainfall for the different SOI phases are likely to impact crop water-stress pattern and yield, and also the type of genotype and management best suited for specific adaptation.

The impacts of SOI phases (calculated in March–April) for the upcoming 'winter' season (May to October) were weaker than climate variations observed during the previous 'summer' (Figure 2 and Figures S1–S8). In 'winter', differences in temperatures were forecasted for most sites with a tendency for greater differences in the northern sites (e.g., Emerald, Roma, and Meandarra), with highest temperatures for SOI phases I & III, and lowest for SOI phases II & IV (Figure 2B and Figures S4–S6). In any case, monthly temperatures of any SOI phases differed by less than 0.5 °C compared to 'all years' (data not shown, Figure 2A and Figures S4–S6). The impact of SOI phases on rainfall was only visible for a few sites, and mainly for higher rainfall in SOI phase IV years (data not shown, Figure 2B and Figure S8). As found in previous studies (e.g., [34]), ENSO had a substantial

impact in northern sites, while a relatively weak impact in southern sites (data not presented for sites south of Condobolin).

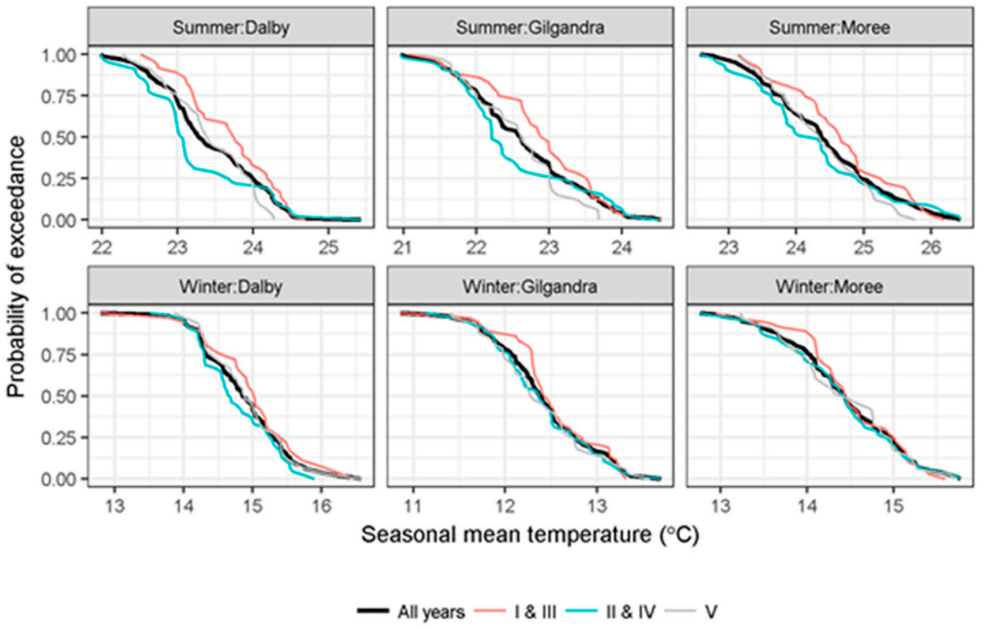

(**A**)

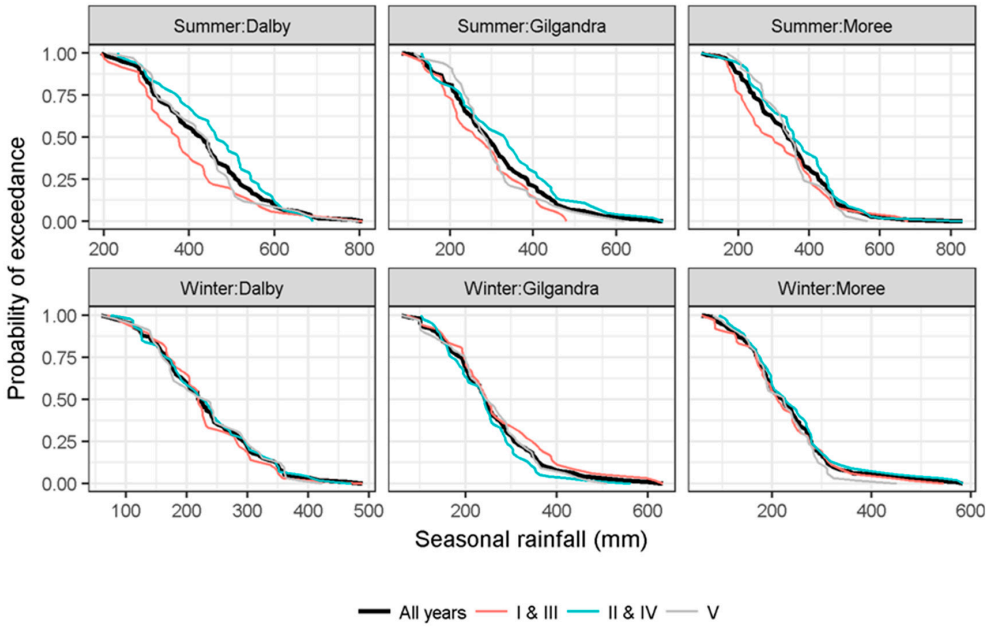

(**B**)

Figure 2. Cumulative probability distributions (probability of exceedance) of 'summer' and 'winter' average temperature (**A**) and cumulated rainfall (**B**) for the three SOI classes, singly (SOI phases I & III, SOI phases II & IV, and SOI phase V) and combined ('all years') for 1900–2016 at three sites in the Eastern wheatbelt. The three SOI classes correspond to SOI consistently negative and rapidly failing (phases I & III), SOI consistently positive and rapidly rising (phases II & IV), and SOI consistently near zero (phase V). SOI phases were determined in March–April, prior to sowing. The 'summer' data were recorded from the previous November to April, while 'winter' data are for the up-coming May to October period. See Figures S1–S8 for average, minimum and maximum temperature, and cumulated rainfall at other sites for both the 'summer' and 'winter' periods.

3.2. ENSO Impacts the Frequency of Occurrence of Frost and Heat Events around Flowering

Extreme temperatures can greatly decrease yield by affecting reproductive organs or impacting grain filling [11,12]. Australian wheat farmers manage their crops to minimise the risk of frost, heat, and drought by targeting the flowering time into an optimum window [7,25]. The last frost day with a 10% risk of frost tended to be earlier in SOI phases II & IV, and delayed in SOI phases I & III mostly in the eastern sites (Figure S9). By contrast, the first heat day with a 30% risk of heat tended to be earlier in SOI phases I & III, and delayed in SOI phases II & IV. Hence, in terms of temperature, the low-risk flowering window tended to last longer for SOI phases II & IV, while it tended to be reduced for SOI phases I & III. Using the three ENSO phases (i.e., El Niño, La Niña and Neutral), Alexander and Hayman [35] found similar trends for distribution and tails of last frost day in 15 sites across the Australian wheatbelt.

3.3. Variations in Yield across SOI Phases

For the reference cultivar and management (i.e., baseline simulations: Janz sown 21 May with farmer fertilisation practices), long-term average yield ranged from 0.93 to 2.71 t·ha^{-1} across sites and averaged 2.06 t·ha^{-1} among the 15 studied sites (Figure 3; 'all years'). Greatest yields were achieved in SOI phases II & IV, with long-term average yield ranging from 0.98 to 2.70 t·ha^{-1} across locations and averaging 2.10 t·ha^{-1} for Eastern Australia. By contrast, long-term average yield in the SOI phases I & III were commonly lower, ranging from 0.90 to 2.70 t·ha^{-1} across locations, and averaging 2.00 t·ha^{-1} for Eastern Australia. Strong links between wheat yield with ENSO were also found in the Eastern wheatbelt in other studies [18,36]. While the early study of Rimmington et al. [37] suggested little impact of ENSO types on wheat yields in Southern and Western Australia, more recent studies found wheat yields to be affected by ENSO in Southern and South-eastern Australia [38,39].

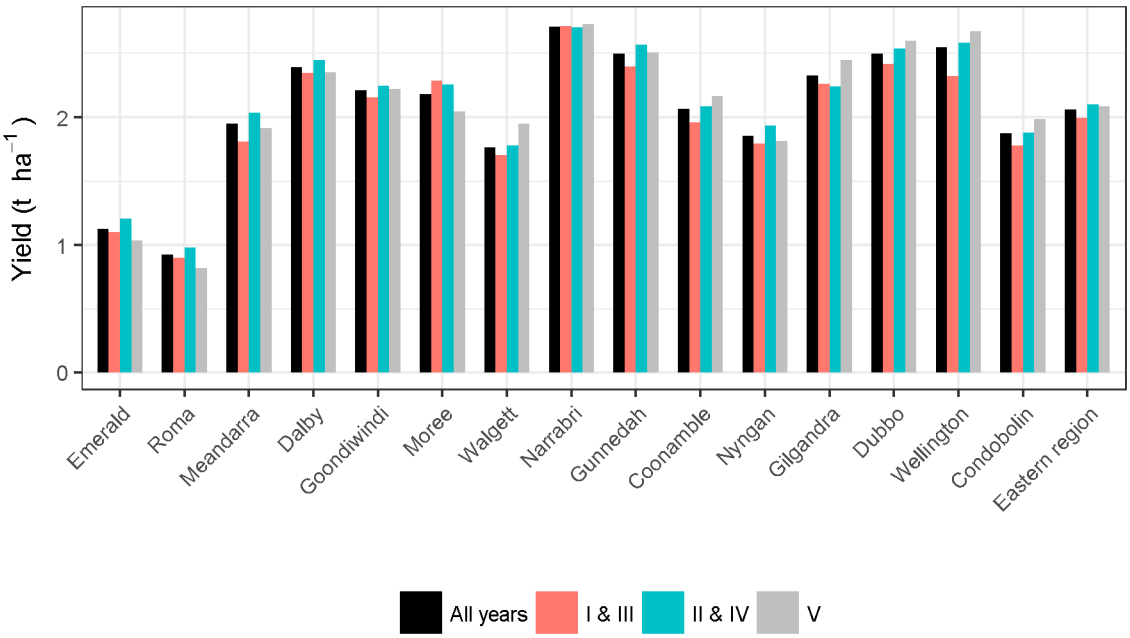

Figure 3. Simulated average yield in the baseline scenario for all years (1900–2016) and for years from each of the three SOI classes at 15 sites across the Eastern wheatbelt and for the whole Eastern wheatbelt region. Baseline simulations corresponded to a standard farmer practice (a medium-season cultivar Janz was sown at semi-optimum sowing date (21 May) with current fertilisation practice). The three SOI classes correspond to SOI consistently negative and rapidly failing (SOI phases I & III), SOI consistently positive and rapidly rising (SOI phases II & IV), and SOI consistently near zero (SOI phase V). SOI phases were determined in March–April, prior to sowing.

3.4. Optimising Genotype and Management across All Years Results in Consistent Yield Improvement and Higher Gross Margins

A large number of adaptation strategies were simulated, combining a wide range of genotypes (with all potential phenology range for Australian wheat) and diverse management practices (a broad range of sowing dates and nitrogen fertilisation options). These strategies were first applied to optimise average yield for a site across all years ('fixed adaptation') by selecting the top yielding genotype × management combination (Figure 4, Figure 5 and Figure S10).

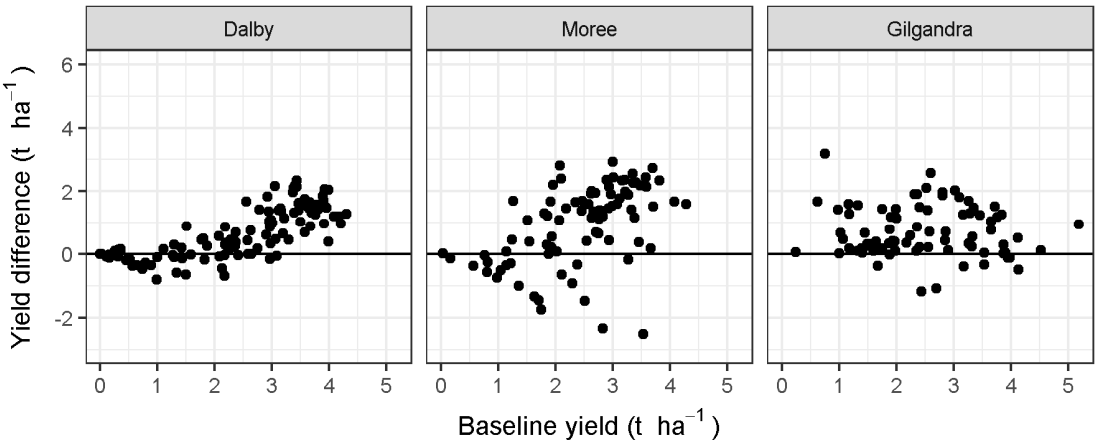

Figure 4. Yield advantage of fixed adaptation over the baseline scenario. The yield difference is calculated for each year. The baseline corresponds to simulated yield for a medium-season cultivar Janz sown at semi-optimum sowing date (21 May) with current fertilisation practice. See Figure S10 for other sites.

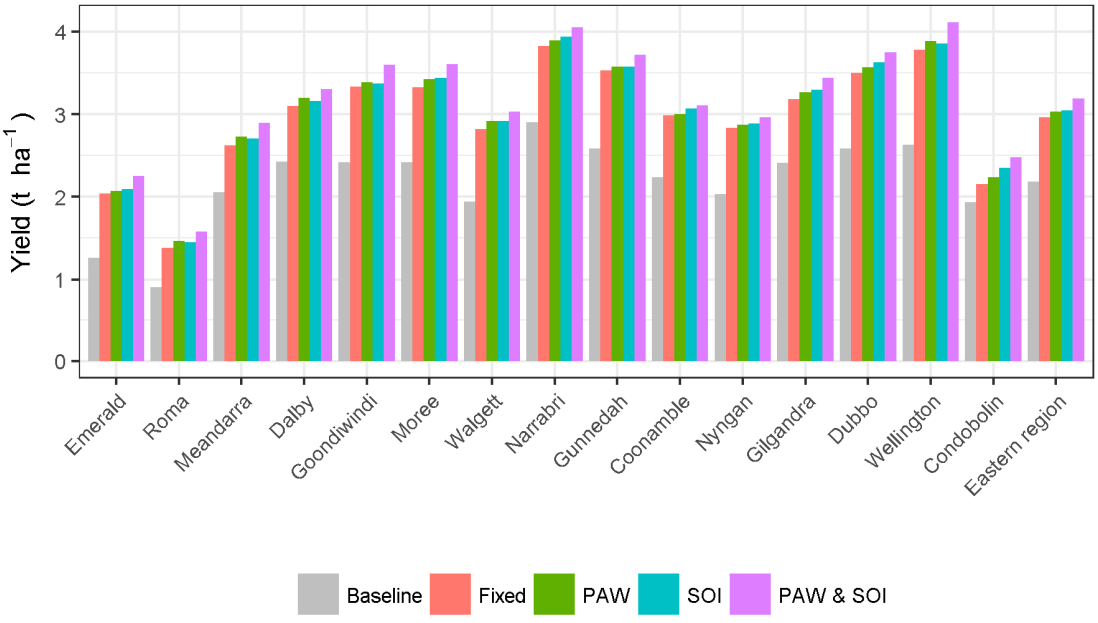

Figure 5. Simulated mean yields for the baseline, fixed adaption, and all the studied tactical adaptation scenarios related to pre-sown soil water and SOI forecast. The baseline corresponds to simulated yield for a medium-season cultivar Janz sown at semi-optimum sowing date (21 May) with no extra nitrogen input. The fixed adaptation scenario corresponds to optimised genotype and management across all years for each site. The three tactical adaptation scenarios include specific adaptation to soil PAW (plant available water) groups, SOI classes, and PAW & SOI groups. These adaptations correspond to optimised genotype and management for each PAW group and/or SOI class. SOI phases were determined in March–April, prior to sowing.

Compared to the baseline, the fixed adaptation scenario increased yields in the majority of years in all sites, although yield losses were also observed for a few years in all sites (Figure 4 and Figure S10). Regional yield (average across all sites) thus increased from 2.06 (baseline) to 2.96 t·ha^{-1} (fixed adaptation) (Figure 5). At the site level, long-term average yield ranged from 1.38 to 3.82 t·ha^{-1} for fixed adaptation compared to 0.91 to 2.90 t·ha^{-1} for the baseline, meaning a yield increase from 0.22 to 1.15 t·ha^{-1} (0.78 t·ha^{-1} on average for the whole region; Figure 3). Compared to the baseline, the fixed adaptation strategy corresponded to an earlier sowing with more nitrogen application of, in general, a shorter-maturing genotype in the northern part of the region, and a longer-maturing genotype in the southern part of the region (data not shown).

In terms of gross margin, site long-term increases from the baseline to fixed adaptation scenario ranged from AU$ 40.5 to 223.0 ha^{-1}, which corresponds to a regional increase of AU$ 153.00 ha^{-1} on average for the whole region. Across Eastern Australia, fixed adaptation resulted in an AU$ 440.00 M increase in gross margin compared to the standard current practice considered here.

3.5. Benefits of Tactical Compared to Fixed Adaptation Vary with the Location, the Soil Pre-Sowing Conditions and the SOI Forecast

To explore the potential of tactical adaptation over fixed adaptation, the genotype and management were optimised for pre-sowing PAW- and/or SOI-specific conditions, and then compared to the fixed adaptation scenario. For most sites (Figure 5), slight increases in long-term average yield were simulated when adapting the genotype and management to either pre-sown PAW or SOI solely. Substantial improvements occurred when optimising average yield for both the genotype and the management for each SOI class and PAW group together (PAW & SOI), rather than sole optimisation of either the PAW group or SOI class. It can nevertheless be noted that fewer of the 117 seasons were classified in each of the nine PAW & SOI groups than in each of three PAW groups or the three SOI classes, meaning that the optimised yield is prone to more uncertainty due to the likely reduction in environmental variations within groups of years considered.

However, tactical adaptation scenarios only allowed yield to increase for some of the years compared to the fixed adaptation (Figure 6 and Figures S11–S13). Actually, when adapting the PAW group only ('PAW adaptation'), losses in yield compared to the fixed adaptation occurred relatively frequently, with losses that were typically small, but which could be as substantial as 2 t·ha^{-1} in some locations (Figure 6 and Figure S11). Similar trends and extents were observed for adaption to SOI classes. Adapting to both PAW and SOI tended to increase the frequency of yield gains, especially in poor seasons (i.e., when yield was medium to low in the fixed adaptation scenario), mainly due to better tuning of the crop phenology (maturity type × sowing time) to the considered environmental conditions. However, yield losses compared to the fixed adaptation still occurred frequently in locations such as Wellington, while they were relatively rare in locations like Coonamble and Moree (Figure S13). Note that the unbalanced number of years among PAW groups, SOI classes, and PAW × SOI groups might cause bias in the adaptation values and risks.

Overall, when considering the optimised genotypes and management for each PAW group ('PAW'), long-term average yield and gross margin increased at each site from 0.012 to 0.13 t·ha^{-1}, and from AU$ 2.63 to 41.9 ha^{-1}, respectively, compared to the fixed adaptation scenario (Figure 7). When considering genotype and management practices optimised for each SOI class ('SOI'), long-term average yield and gross margin at each site increased from 0.037 to 0.17 t·ha^{-1}, and from AU$ 5.00 to 41.50 ha^{-1}, respectively. Finally, when considering optimised management and cultivar for each combination of PAW group and SOI class ('PAW & SOI'), average yield and gross margin at each site increased from 0.15 to 0.46 t·ha^{-1}, and from AU$ 34.2.00 to 108 ha^{-1}, respectively, compared to the fixed adaptation. Hammer et al. (1996) studied the adapted values of SOI phases through changing cultivars and nitrogen fertilisation at Goondiwindi, and also found a substantial, although more limited, increase in gross margin ($26 ha^{-1}) compared with results in this study ($48 ha^{-1}, Figure 7B) [1].

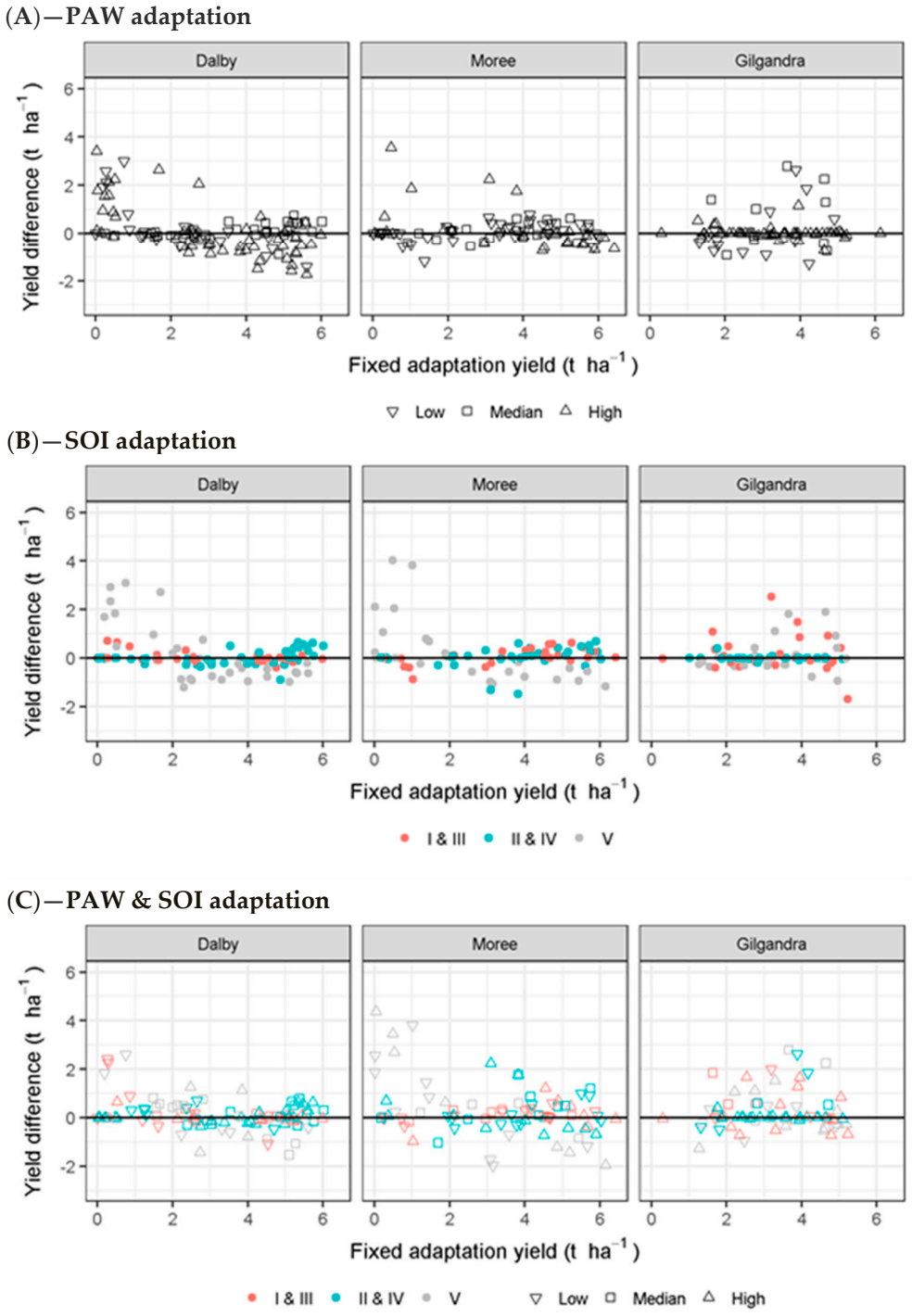

Figure 6. Yield advantage of tactical adaptation scenarios for (**A**) pre-sowing soil PAW (low, median and high), (**B**) SOI classes (I & III, II & IV and V), and (**C**) both PAW & SOI groups over fixed adaptation. The yield difference is calculated for each year. The fixed adaptation scenario corresponds to optimised genotype and management across all years. The three tactical adaptation scenarios correspond to optimised genotype and management for each PAW (plant available water) group and/or SOI class. SOI phases were determined in March–April, prior to sowing. See Figures S11–S13 for other sites.

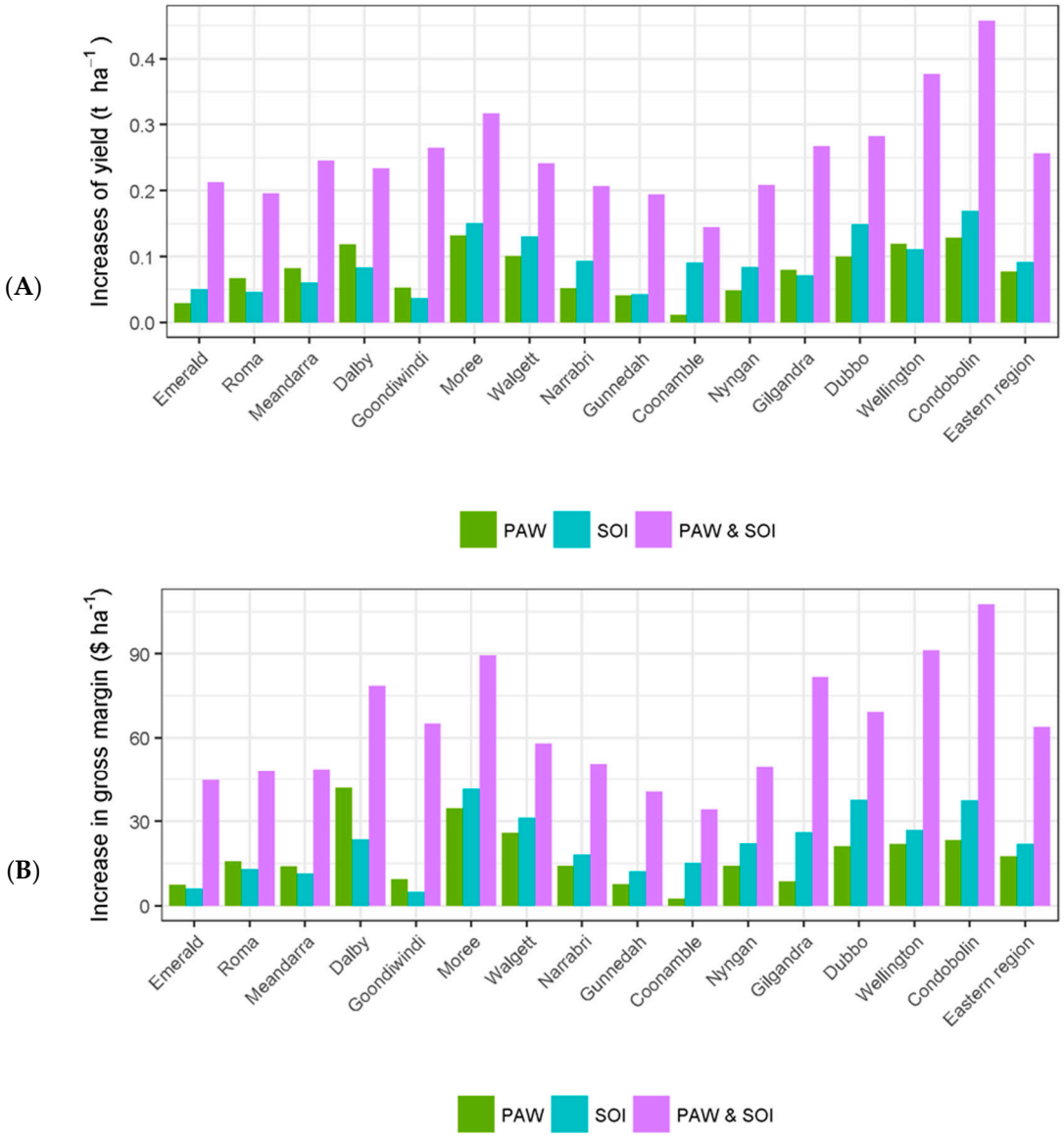

Figure 7. Increase in simulated yield (**A**) and gross margin (**B**) for tactical adaptation options compared to the fixed adaptation in each studied site and the whole Eastern wheatbelt. Increases in yield were averaged for all years from 1900 to 2016. The three tactical adaptation options correspond to optimise long-term yield for either (i) low/medium/high pre-sowing plant available water (PAW), (ii) each class of Southern Oscillation Index (SOI), or (iii) each combination of PAW group and SOI class.

At the regional scale, long-term mean increased in yield and gross margin of PAW & SOI tactical adaptation versus fixed adaptation were 0.26 t·ha^{-1} and AU$ 63.90 ha^{-1}, respectively. The cumulated regional increase in gross margin was AU$ 188 M for the Eastern wheatbelt. Note that the increase gross margin in this paper considered fixed nitrogen price, and accounted for neither changing wheat price related to the harvested grain quality, nor to the domestic and/or global market.

3.6. Should Eastern Australian Wheat Producers Adapt Their Decisions Based on SOI Phases?

In Australia, SOI phases impact the climate and crops mostly in the eastern part of the wheatbelt. In this region, wheat management occurs almost exclusively at sowing. While specific adaptation could be more accurate later in the season, i.e., when climate trends in regard to El Niño/La Niña are clearer, early forecast of the SOI phases is required to allow farmers to prepare seeds and plan suitable management. The potential gains of specific adaptation to such pre-sowing forecasts of SOI phases

combined with knowledge on initial soil water appeared to be substantial (Figures 5 and 7). While the gains are variable depending on the location, the extra costs for seed companies and farmers to store large stocks of seeds required for specific adaptation may have to be considered, especially at the farm scale. Unpredictable rainfall in the autumn before sowing may also constrain sowing opportunities [1]. That said, the potential gains of specific adaptation appear to be well above what could be expected from most breeding innovations, at least in the short term [40].

Other methods exist to forecast short-term or seasonal climate. For instance, the Australian Bureau of Meteorology produced twice-weekly weather forecasts for a period of 270 days, with a dynamic model called POAMA (http://poama.bom.gov.au/info/poama-2.html) [41–43]. Such seasonal forecasts have been used to look at management strategies of crops [44–46]. To improve these forecasts, which use on a grid of about 250 km, the Bureau of Meteorology is now proposing seasonal forecasts (ACCESS-S) based on ACCESS (Australian Community Climate and Earth System Simulator; http://www.bom.gov.au/australia/charts/about/about_access.shtml) using a 60 km grid. Other indices than SOI or ENSO phases could also be used for specific adaptation, such as the Inter-decadal Pacific Oscillation (IPO) phases [47] or drought environmental types [20,22,48,49] if climate forecasts are sufficiently reliable. For instance, crop models have been used to assess the value of broad and specific adaptations to select sorghum varieties and managements for different types of drought environments [20].

4. Conclusions

In this study, we assessed the value of fixed adaptation (no distinction between the years) and tactical adaptations based on pre-sowing plant available water (PAW) and/or SOI forecasts to increase productivity at given sites. Overall, with our current knowledge, it appears that yield gains can be made from improving cultivar and management strategy both regardless of climate forecast (fixed adaptation), and as a tactical adaptation to pre-sowing soil water conditions and climate forecasts. The benefits of PAW and SOI tactical adaptation could be useful for farmers to adjust farm management practices according to the season, and may be improved with new forecasting climate methods such as the newly developed ACCESS-S model.

Supplementary Materials: The following are available online at http://www.mdpi.com/2225-1154/6/3/77/s1. Figure S1: Cumulative probability distributions of 'summer' average temperature for the three SOI classes, singly and combined ('all years'), Figure S2: Cumulative probability distributions of 'summer' maximum temperature for the three SOI classes, singly and combined ('all years'), Figure S3: Cumulative probability distributions of 'summer' minimum temperature for the three SOI classes, singly and combined ('all years'), Figure S4: Cumulative probability distributions of 'winter' average temperature for the three SOI classes, singly and combined ('all years'), Figure S5: Cumulative probability distributions of 'winter' maximum temperature for the three SOI classes, singly and combined ('all years'), Figure S6: Cumulative probability distributions of 'winter' minimum temperature for the three SOI classes, singly and combined ('all years'), Figure S7: Cumulative probability distributions of 'summer' total rainfall for the three SOI classes, singly and combined ('all years'), Figure S8: Cumulative probability distributions (probability of exceedance) of 'winter' total rainfall for the three SOI classes, singly and combined ('all years'), Figure S9: Probability of last frost day and first heat day for the three SOI classes, singly and combined ('all years'), Figure S10: Simulated yield advantage of fixed adaptation over the baseline scenario, Figure S11: Simulated yield advantage of PAW tactical adaptation scenario over fixed adaptation scenario, Figure S12: Simulated yield advantage of SOI tactical adaptation scenario over fixed adaptation scenario, Figure S13: Simulated yield advantage of PAW & SOI tactical adaptation scenario over fixed adaptation scenario.

Author Contributions: B.Z., S.C. and K.C. conceived and developed the ideas; B.Z. and K.C. performed the data analysis; B.Z., S.C. and K.C. wrote the paper.

Funding: This research received no external funding.

Acknowledgments: This research was funded by the CSIRO and the University of Queensland.

Conflicts of Interest: The authors declare no conflict of interest.

References

1. Hammer, G.L.; Holzworth, D.P.; Stone, R. The value of skill in seasonal climate forecasting to wheat crop management in a region with high climatic variability. *Aust. J. Agric. Res.* **1996**, *47*, 717–737. [CrossRef]
2. Chapman, S.C.; Chakraborty, S.; Dreccer, M.F.; Howden, S.M. Plant adaptation to climate change? Opportunities and priorities in breeding. *Crop Pasture Sci.* **2012**, *63*, 251–268. [CrossRef]
3. Potgieter, A.B.; Hammer, G.L.; Butler, D. Spatial and temporal patterns in Australian wheat yield and their relationship with ENSO. *Aust. J. Agric. Res.* **2002**, *53*, 77–89. [CrossRef]
4. Meinke, H.; de Voil, P.; Hammer, G.L.; Power, S.; Allan, R.; Stone, R.C.; Folland, C.; Potgieter, A. Rainfall Variability at Decadal and Longer Time Scales: Signal or Noise? *J. Clim.* **2005**, *18*, 89–96. [CrossRef]
5. Yates, D.; Vervoort, R.W.; Minasny, B.; McBratney, A. The history of using rainfall data to improve production in the grain industry in Australia—From Goyder to ENSO. *Crop Pasture Sci.* **2016**, *67*, 467–479. [CrossRef]
6. Chenu, K.; Cooper, M.; Hammer, G.L.; Mathews, K.L.; Dreccer, M.F.; Chapman, S.C. Environment characterization as an aid to wheat improvement: Interpreting genotype–environment interactions by modelling water-deficit patterns in North-Eastern Australia. *J. Exp. Bot.* **2011**, *62*, 1743–1755. [CrossRef] [PubMed]
7. Zheng, B.Y.; Chenu, K.; Dreccer, M.F.; Chapman, S.C. Breeding for the future: What are the potential impacts of future frost and heat events on sowing and flowering time requirements for Australian bread wheat (*Triticum aestivum*) varieties? *Glob. Chang. Biol.* **2012**, *18*, 2899–2914. [CrossRef] [PubMed]
8. Nicholls, N.; Baek, H.J.; Gosai, A.; Chambers, L.E.; Choi, Y.; Collins, D.; Della-Marta, P.M.; Griffiths, G.M.; Haylock, M.R.; Iga, N.; et al. The El Niño–Southern Oscillation and daily temperature extremes in East Asia and the west Pacific. *Geophys. Res. Lett.* **2005**, *32*, L16714. [CrossRef]
9. Chambers, L.E.; Griffiths, G.M. The changing nature of temperature extremes in Australia and New Zealand. *Aust. Meteorol. Mag.* **2008**, *57*, 13–35.
10. Lobell, D.B.; Hammer, G.L.; Chenu, K.; Zheng, B.; McLean, G.; Chapman, S.C. The shifting influence of drought and heat stress for crops in Northeast Australia. *Glob. Chang. Biol.* **2015**, *21*, 4115–4127. [CrossRef] [PubMed]
11. Frederiks, T.M.; Christopher, J.T.; Harvey, G.L.; Sutherland, M.W.; Borrell, A.K. Current and emerging screening methods to identify post-head-emergence frost adaptation in wheat and barley. *J. Exp. Bot.* **2012**, *63*, 5405–5416. [CrossRef] [PubMed]
12. Zheng, B.; Chapman, S.C.; Christopher, J.T.; Frederiks, T.M.; Chenu, K. Frost trends and their estimated impact on yield in the Australian wheatbelt. *J. Exp. Bot.* **2015**, *66*, 3611–3623. [CrossRef] [PubMed]
13. Crimp, S.J.; Zheng, B.; Khimashia, N.; Gobbett, D.L.; Chapman, S.; Howden, M.; Nicholls, N. Recent changes in southern Australian frost occurrence: Implications for wheat production risk. *Crop Pasture Sci.* **2016**, *67*, 801–811. [CrossRef]
14. Timmermann, A.; Oberhuber, J.; Bacher, A.; Esch, M.; Latif, M.; Roeckner, E. Increased El Nino frequency in a climate model forced by future greenhouse warming. *Nature* **1999**, *398*, 694–697. [CrossRef]
15. Cai, W.; Wang, G.; Santoso, A.; McPhaden, M.J.; Wu, L.; Jin, F.-F.; Timmermann, A.; Collins, M.; Vecchi, G.; Lengaigne, M.; et al. Increased frequency of extreme La Nina events under greenhouse warming. *Nat. Clim. Chang.* **2015**, *5*, 132–137. [CrossRef]
16. McPhaden, M.J.; Zebiak, S.E.; Glantz, M.H. ENSO as an Integrating Concept in Earth Science. *Science* **2006**, *314*, 1740–1745. [CrossRef] [PubMed]
17. Ashok, K.; Yamagata, T. Climate change: The El Nino with a difference. *Nature* **2009**, *461*, 481–484. [CrossRef] [PubMed]
18. Stone, R.; Hammer, G.L.; Marcussen, T. Prediction of global rainfall probabilities using phases of the Southern Oscillation Index. *Nature* **1996**, *384*, 252–255. [CrossRef]
19. Hammer, G.L.; McLean, G.; Chapman, S.; Zheng, B.; Doherty, A.; Harrison, M.T.; van Oosterom, E.; Jordan, D. Crop design for specific adaptation in variable dryland production environments. *Crop Pasture Sci.* **2014**, *65*, 614–626.
20. Stone, R.; Nicholls, N.; Hammer, G. Frost in Northeast Australia: Trends and influences of phases of the Southern Oscillation. *J. Clim.* **1996**, *9*, 1896–1909. [CrossRef]
21. Woli, P.; Ortiz, B.V.; Johnson, J.; Hoogenboom, G. El Niño–Southern Oscillation Effects on winter wheat in the southeastern United States. *Agron. J.* **2015**, *107*, 2193. [CrossRef]

22. Chenu, K.; Deihimfard, R.; Chapman, S.C. Large-scale characterization of drought pattern: A continent-wide modelling approach applied to the Australian wheatbelt—Spatial and temporal trends. *New Phytol.* **2013**, *198*, 801–820. [CrossRef] [PubMed]
23. Dennett, M.D. Effects of sowing date and the determination of optimum sowing date. In *Wheat: Ecology and Physiology of Yield Determination*; Satorre, E.H., Slafer, G.H., Eds.; Food Products Press: Binghamton, NY, USA, 1999; pp. 123–140.
24. Pook, M.; Lisson, S.; Risbey, J.; Ummenhofer, C.C.; McIntosh, P.; Rebbeck, M. The autumn break for cropping in southeast Australia: Trends, synoptic influences and impacts on wheat yield. *Int. J. Climatol.* **2009**, *29*, 2012–2026. [CrossRef]
25. Flohr, B.M.; Hunt, J.R.; Kirkegaard, J.A.; Evans, J.R. Water and temperature stress define the optimal flowering period for wheat in south-eastern Australia. *Field Crops Res.* **2017**, *209*, 108–119. [CrossRef]
26. Chenu, K.; Porter, J.R.; Martre, P.; Basso, B.; Chapman, S.C.; Ewert, F.; Bindi, M.; Asseng, S. Contribution of Crop Models to Adaptation in Wheat. *Trends Plant Sci.* **2017**, *22*, 472–490. [CrossRef] [PubMed]
27. Holzworth, D.P.; Huth, N.; de Voil, P.G.; Zurcher, E.J.; Herrmann, N.I.; McLean, G.; Chenu, K.; Van Oosterom, E.; Murphy, C.; Moore, A.D.; et al. APSIM—Evolution towards a new generation of agricultural systems simulation. *Environ. Model. Softw.* **2014**, *62*, 327–350. [CrossRef]
28. Zheng, B.Y.; Biddulph, B.; Li, D.; Kuchel, H.; Chapman, S.C. Quantification of the effects of *VRN1* and *Ppd-D1* to predict spring wheat (*Triticum aestivum*) heading time across diverse environments. *J. Exp. Bot.* **2013**, *64*, 3747–3761. [CrossRef] [PubMed]
29. Jeffrey, S.J.; Carter, J.O.; Moodie, K.B.; Beswick, A.R. Using spatial interpolation to construct a comprehensive archive of Australian climate data. *Environ. Model. Softw.* **2001**, *16*, 309–330. [CrossRef]
30. Zheng, B.; Chenu, K.; Doherty, A.; Chapman, S. *The APSIM-Wheat Module (7.5 R3008)*; Agricultural Production Systems Simulator (APSIM) Initiative: Toowoomba, Australian, 2014.
31. Christopher, J.T.; Christopher, M.J.; Borrell, A.K.; Fletcher, S.; Chenu, K. Stay-green traits to improve wheat adaptation in well-watered and water-limited environments. *J. Exp. Bot.* **2016**, *67*, 5159–5172. [CrossRef] [PubMed]
32. Zheng, B.; Holland, E.; Chapman, S.C. A standardized workflow to utilise a grid-computing system through advanced message queuing protocols. *Environ. Model. Softw.* **2016**, *84*, 304–310. [CrossRef]
33. Australian Bureau of Agricultural and Resource Economics (ABARE). *Australian Commodity Statistics 2016*; ABARE: Canberra, Australia, 2016.
34. Stone, R.; Auliciems, A. SOI phase relationships with rainfall in eastern Australia. *Int. J. Climatol.* **1992**, *12*, 625–636. [CrossRef]
35. Alexander, B.; Hayman, P. Can we use forecasts of El Nino and La Nina for frost management in the Eastern and Southern grains belt? In Proceedings of the 14th Agronomy Conference, Adelaide, Australia, 21–25 September 2008.
36. Potgieter, A.B.; Hammer, G.L.; Meinke, H.; Stone, R.C.; Goddard, L. Three putative types of El Niño revealed by spatial variability in impact on Australian wheat yield. *J. Clim.* **2005**, *18*, 1566–1574. [CrossRef]
37. Rimmington, G.M.; Nicholls, N. Forecasting wheat yields in Australia with the Southern Oscillation Index. *Crop Pasture Sci.* **1993**, *44*, 625–632. [CrossRef]
38. Anwar, M.R.; Rodriguez, D.; Liu, D.L.; Power, S.; O'Leary, G.J. Quality and potential utility of ENSO-based forecasts of spring rainfall and wheat yield in south-eastern Australia. *Crop Pasture Sci.* **2008**, *59*, 112–126. [CrossRef]
39. Hayman, P.T.; Whitbread, A.M.; Gobbett, D.L. The impact of El Niño Southern Oscillation on seasonal drought in the southern Australian grainbelt. *Crop Pasture Sci.* **2010**, *61*, 528–539. [CrossRef]
40. Marshall, G.R.; Parton, K.A.; Hammer, G.L. Risk attitude, planting conditions and the value of seasonal forecasts to a dryland wheat grower. *Aust. J. Agric. Econ.* **1996**, *40*, 211–233. [CrossRef]
41. Zhao, M.; Hendon, H.H. Representation and prediction of the Indian Ocean dipole in the POAMA seasonal forecast model. *Q. J. R. Meteorol. Soc.* **2009**, *135*, 337–352. [CrossRef]
42. Marshall, A.G.; Hudson, D.; Hendon, H.H.; Pook, M.J.; Alves, O.; Wheeler, M.C. Simulation and prediction of blocking in the Australian region and its influence on intra-seasonal rainfall in POAMA-2. *Clim. Dyn.* **2014**, *42*, 3271–3288. [CrossRef]
43. Hudson, D.; Marshall, A.G.; Yin, Y.; Alves, O.; Hendon, H.H. Improving intraseasonal prediction with a new ensemble generation strategy. *Mon. Weather Rev.* **2013**, *141*, 4429–4449. [CrossRef]

44. Asseng, S.; McIntosh, P.C.; Wang, G.; Khimashia, N. Optimal N fertiliser management based on a seasonal forecast. *Eur. J. Agron.* **2012**, *38*, 66–73. [CrossRef]
45. Hayman, P.; Cooper, B.; Parton, K.; Alves, O.; Yong, G.; Henry, H.; Scheer, C. Can advances in climate forecasts improve the productive and environmental outcomes from nitrogen fertiliser on wheat? A case study using POAMA for topdressing wheat in South Australia. In Proceedings of the 17th Australian Agronomy Conference, Hobart, Tasmania, 20–24 September 2015; Australian Society of Agronomy: Hobart, Australia, 2015.
46. Rodriguez, D.; de Voil, P.; Hudson, D.; Brown, J.N.; Hayman, P.; Marrou, H.; Meinke, H. Predicting optimum crop designs using crop models and seasonal climate forecasts. *Sci. Rep.* **2018**, *8*, 2231. [CrossRef] [PubMed]
47. Power, S.; Casey, T.; Folland, C.; Colman, A.; Mehta, V. Inter-decadal modulation of the impact of ENSO on Australia. *Clim. Dyn.* **1999**, *15*, 319–324. [CrossRef]
48. Chapman, S.C.; Cooper, M.; Hammer, G.L. Using crop simulation to generate genotype by environment interaction effects for sorghum in water-limited environments. *Aust. J. Agric. Res.* **2002**, *53*, 379–389. [CrossRef]
49. Chenu, K. Characterizing the crop environment—Nature, significance and applications. In *Crop Physiology. Applications for Genetic Improvement and Agronomy*; Sadras, V.O., Calderini, D., Eds.; Academic Press: London, UK, 2015; pp. 321–348. ISBN 978-0-12-417104-6.